ELSEVIER

Journal of Magnetism and Magnetic Materials 252 (2002) 13–15

journal of magnetism and magnetic materials

www.elsevier.com/locate/jmmm

Investigation of magnetic nanoparticles in acrylonitrile-methyl methacrylate-divinylbenzene mesoporous template

D. Rabelo[a,*], E.C.D. Lima[a], D.P. Barbosa[a], V.J. Silva[a], O. Silva[b], R.B. Azevedo[c], L.P. Silva[c], A.P.C. Lemos[c], P.C. Morais[d]

[a] *Instituto de Química, Universidade Federal de Goiás, Goiânia-GO 74001-970, Brazil*
[b] *Instituto de Física, Universidade Federal de Goiás, Goiânia-GO 74001-970, Brazil*
[c] *Instituto de Ciências Biológicas, Universidade de Brasília, Brasília-DF 70910-900, Brazil*
[d] *Instituto de Física, Universidade de Brasília, Núcleo de Física Aplicada, Brasília-DF 70919-970, Brazil*

Abstract

Preparation and characterization of nanosized magnetic particles using alkaline oxidation of ferrous ion retained in acrylonitrile-methyl methacrylate-divinylbenzene (AN-MMA-DVB) spherical micron-sized polymer template is described. Atomic absorption, transmission electron microscopy and magnetic resonance were used to investigate chemically cycled nanoparticle-based composites. The resonance field shifts towards higher values as the nanoparticle concentration reduces in the polymeric template, following two very distinct regimes.

Keywords: Fine particles; Particles—size distribution; Resonance—magnetic; Transmission electron microscopy

The design/synthesis of nanometer-sized magnetic particles in micron-sized polymeric templates has attracted a lot of attention [1,2]. Micron-sized magnetic particles are currently in use, for instance, in high-gradient magnetic separation (HGMS) devices [3,4]. Characterization of nanomagnetic-based composites has been performed by traditional techniques, e.g., magnetometry and Mössbauer spectroscopy [5]. Magnetic resonance (MR), however, has been used to investigate nanomagnetic particles immersed in a wide variety of non-magnetic matrices [6–9]. In this study, atomic absorption (AA), transmission electron microscopy (TEM) and MR were used to investigate iron oxide-based magnetic nanoparticles immersed in acrylonitrile-methyl methacrylate-divinylbenzene (AN-MMA-DVB) spherical micron-sized polymer template.

Incorporation of the magnetic material in the polymeric template was performed by treating the template with Fe^{2+} aqueous solution (bath solution) at a concentration of 80 mM (first step) following oxidation (second step) with a mixture of KOH and KNO_3, according to the standard recipe used to produce magnetite crystals [10]. Six composite samples were prepared using successive treatments with the bath solution, following the oxidation step. The amount of magnetic material incorporated in the template as a function of the number of treatments (cycles) was obtained from AA measurements. In the six composite samples, TEM was used to obtain the particle size polydispersity profiles of the nanomagnetic material. Room-temperature MR measurements of the six composite samples were also carried out.

Filled circles in Fig. 1 show the total iron incorporation in the template, M, obtained from the AA data, after performing the second step, in units of mmol of iron per unit gram of the initial copolymer template, as a function of the number of cycles, N. The rate at which iron is incorporated in the polymer template, i.e. dM/dN, can be given by $K(M_0 - M)$ [5]. Therefore, M versus N can be obtained by solving the differential equation $dM/dN = K(M_0 - M)$, i.e.

*Corresponding author.
E-mail address: denilson@quimica.ufg.br (D. Rabelo).

0304-8853/02/$ - see front matter
PII: S0304-8853(02)00692-3

$M = M_0\{1 - \exp[-K(N - N_0)]\}$. The parameter N_0 was introduced to indicate at which cycle the AA measurements indicate iron incorporation. The solid line in Fig. 1 represents the best fit of the experimental data with $M_0 = 2.2$ mmol/g, $K = 0.06$, and $N_0 = 2$.

Fig. 2 shows the particle size histograms obtained from the TEM images of the $N = 1$ and 6 cycles composite samples. The histograms were curve fitted (solid lines) using the lognormal probability function [11], from which the average particle diameter D and standard deviation σ were obtained (values quoted in Fig. 2). We find D and σ almost independent of N. This finding indicates that successive incorporation of the nanomagnetic material in the template is achieved mostly by increasing the number of particles per unit volume at about fixed particle size.

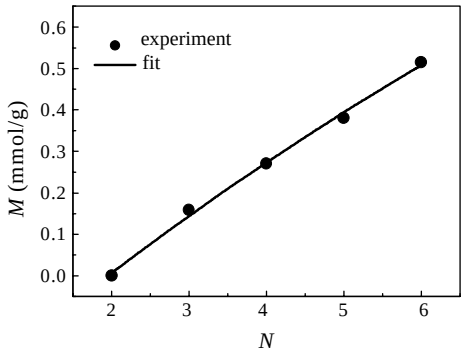

Fig. 1. Total iron incorporation in the polymeric template (M) versus number of cycles (N).

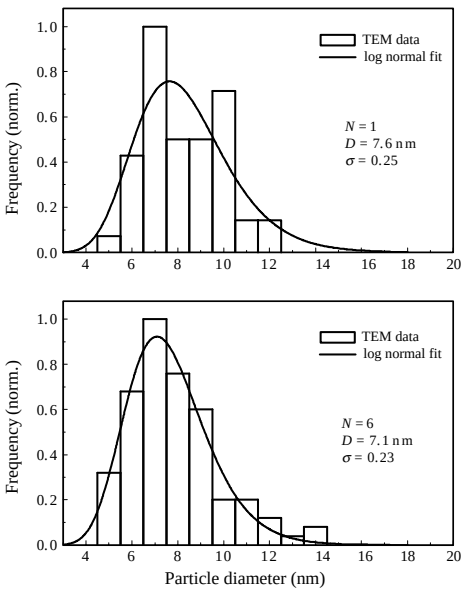

Fig. 2. Particle size histogram (TEM data) of nanoparticles in the composite samples after 1 and 6 cycles.

Room-temperature MR spectra were recorded using a commercial X-band spectrometer. Filled circles in Fig. 3 represent the resonance field (H_R) versus the inverse of the area ($1/A$) under the MR absorption curve. The area (A) scales with the number of nanoparticle per unit volume (C). The explanation of the data shown in Fig. 3 starts using the relationship between the resonance frequency (ω_R) of the nanoparticle magnetic moment and the effective magnetic field (H_{EFF}), $\omega_R = \gamma H_{EFF}$, where γ is the gyromagnetic ratio. At low particle concentration the effective field is mainly a combination of the external field (H_E), the exchange field (H_X), the anisotropy field (H_K), and the demagnetizing field (H_D), i.e. $H_{EFF} = H_E + H_X + H_K + H_D$ [12]. Only the demagnetizing field depends upon the nanoparticle concentration. At the resonance condition, $H_E = H_R$, the basic resonance equation is rewritten as $H_R = H_0 - H_D$, with $H_0 = \omega_R/\gamma - H_X - H_K$. The demagnetizing field of isolated spherical nanoparticles in an inert matrix, however, is given by $H_D = (4\pi/3)[(1/p) - 1]M$, where M is the magnetization associated to the nanomagnetic particle and p is the volumetric packing fraction of the nanomagnetic material [13]. The relationship between p and C is $p = \pi D^3 C/6$, where D is the nanoparticle diameter. Therefore, at low-concentration the relationship between H_R and A would be written as $H_R = h_0 + k_1/A$, where h_0 and k_1 are fitting parameters. The data in Fig. 3, however, shows a linear relationship between H_R and $1/A$ only at N below 6. At $N = 6$ particle–particle (dipole) interaction plays a key role in the H_R versus $1/A$ curve and thus needs to be taken into account.

Inclusion of the particle–particle interaction in the description of the H_R versus $1/A$ curve assumes the following relationship between the resonance field shift (δH_R) and the resonance linewidth (ΔH_R): $\delta H_R \approx \Delta H_R^2$ [14]. Description of the resonance linewidth as a function of the nanoparticle concentration (which scales with A) has been successfully achieved by $\Delta H_R \approx A \tanh(KA^2)$ [15]. Therefore, the description of

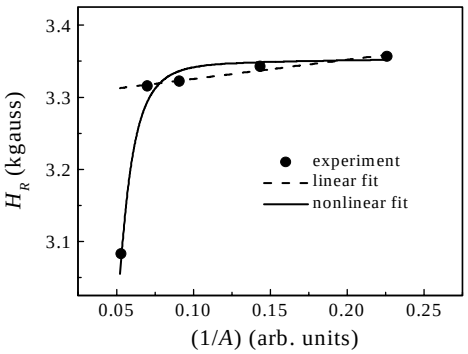

Fig. 3. Resonance field versus the inverse of the area under the absorption resonance curve.

the H_R versus $1/A$ data, including both the demagnetizing field and the particle-particle interaction, reads:

$$H_R = H_0 + K_1/A - K_2A^2 \tanh^2(K_3A^2), \quad (1)$$

where H_0 and K_j ($j = 1, 2, 3$) are fitting parameters. The solid line in Fig. 3 represents the best fit of the data according to Eq. (1). The dashed line in Fig. 3 represents the best fit of the experimental data, for N below 6, using only the two first terms on the right-hand side of Eq. (1).

In summary, different techniques were used to characterize magnetic nanoparticles synthesized in AN-MMA-DVB polymeric template. While atomic absorption and resonance measurements were used to draw conclusions about the amount of magnetic mass incorporation electron microscopy provides very useful information concerning the particle size polydispersity profile. In addition, magnetic resonance data were used to support the picture of an almost linear mass incorporation upon chemical cycling while keeping constant the mean nanoparticle diameter.

Acknowledgements

This work was partially supported by the Brazilian agencies CTPetro, FAP-DF, CNPq, and CAPES.

References

[1] P.A. Dresco, V.S. Zaitsev, R.J. Gambino, B. Chu, Langmuir 15 (1999) 1945.
[2] F.M. Winnik, A. Morneau, A.M. Mika, R.F. Childs, A. Roig, E. Molins, R.F. Ziolo, Can. J. Chem. 76 (1998) 10.
[3] H. Honda, A. Kawabe, A. Shinkai, T.J. Kobayashi, J. Ferment. Bioeng. 86 (1998) 191.
[4] A.D. Ebner, J.A. Ritter, H.J. Ploehn, R.L. Koochen, J.D. Navratil, Sep. Sci. Technol. 34 (1999) 1277.
[5] D. Rabelo, E.C.D. Lima, A.C. Reis, W.C. Nunes, M.A. Novak, V.K. Garg, A.C. Oliveira, P.C. Morais, Nano Lett. 1 (2001) 105.
[6] R. Berger, J.C. Bissey, J. Kliava, B. Soulard, J. Magn. Magn. Mater. 167 (1998) 129.
[7] P.C. Morais, M.C.F.L. Lara, A.L. Tronconi, F.A. Tourinho, A.R. Pereira, F. Pelegrini, J. Appl. Phys. 79 (1996) 7931.
[8] J.F. Saenger, K. Skeff Neto, P.C. Morais, M.H. Sousa, F.A. Tourinho, J. Magn. Res. 134 (1998) 180.
[9] E. Wajnberg, D. Acosta-Avalos, L.J. El-Jaick, L. Abraçado, J.L.A. Coelho, A.F. Bakuzis, P.C. Morais, D.M.S. Esquivel, Biophys. J. 78 (2000) 1018.
[10] S.B. Couling, S. Mann, J. Chem. Soc. Chem. Commun. 0 (1985) 1713.
[11] B.M. Lacava, R.B. Azevedo, L.P. Silva, Z.G.M. Lacava, K. Skeff Neto, N. Buske, A.F. Bakuzis, P.C. Morais, Appl. Phys. Lett. 77 (2000) 1876.
[12] A.F. Bakuzis, P.C. Morais, F. Pelegrini, J. Appl. Phys. 85 (1999) 7480.
[13] E. Kneller, Fine particle theory, in: A.E. Berkowitz, E. Kneller (Eds.), Magnetism and Metallurgy, Vol. 1, Academic Press, New York, 1969, p. 365.
[14] K. Nagata, A. Ishihara, J. Magn. Magn. Mater. 104 (1992) 1571.
[15] P.C. Morais, M.C.F.L. Lara, K. Skeff Neto, Philos. Magn. Lett. 55 (1987) 181.